

Batch and column studies on the removal of methyl orange by *Acalypha indica* biomass using gravitational search algorithm as an optimization tool

V. Aruna Janani^a, S. Saravanan^{a,*}, S. Rajesh^b, P. Sivakumar^c, Sircar Anirbid^c

^aDepartment of Chemical Engineering, Kalasalingam Academy of Research and Education, Krishnankoil 626126, India, Tel. +91 9443271620; Fax: +91 04563289322; email: saravanan.s@klu.ac.in (S. Saravanan), v.arunajanani@klu.ac.in (V.A. Janani)

^bDepartment of Mechanical Engineering, Kalasalingam Academy of Research and Education, Krishnankoil 626126, India, email: s.rajesh@klu.ac.in

^cSchool of Petroleum Technology, Pandit Deendayal Petroleum University, Gandhinagar 382007, India, email: sivakumar.p@spt.pdpu.ac.in (P. Sivakumar), anirbid.sircar@spt.pdpu.ac.in (S. Anirbid)

Received 22 August 2018; Accepted 5 January 2019

ABSTRACT

The biosorption of methyl orange dye from an aqueous solution onto *Acalypha indica* (*A. indica*) was examined using batch and continuous processes. The equilibrium dye uptake limit of *A. indica* was determined by analyzing the impact of different working parameters like adsorbent dose, pH, and time. The biosorbent was exemplified by scanning electron microscopy, Fourier transform infrared spectroscopy, surface area analyzer, point of zero charge, and Boehm titration. In batch experiments, the maximum uptake capacity of sorbent (82 mg g⁻¹) was achieved with the biosorbent dosage of 0.03 g 100 mL⁻¹ and at pH 3.0. Henry's isotherm model was ($R^2 = 0.997$) proved to be a better fit than Langmuir and Freundlich isotherms. The data acquired from kinetic studies were found to fit well with the Elovich's model ($R^2 > 0.99$) when compared with pseudo-first-order, pseudo-second-order equation, and intraparticle diffusion model. Optimized parameters from batch studies were further employed for column studies. Maximum uptake capacity of biosorbent (244 mg g⁻¹) was obtained at the bed height of 3 cm and at the flow rate of 5 mL min⁻¹. Breakthrough curves showed that the chosen biosorbent reduced the concentration of dye from 30 mg L⁻¹ to appreciable level. Gravitational search algorithm (GSA) was employed to predict the optimal combination of the process parameters. It was observed from the GSA results that the equilibrium uptake capacity of the biosorbent should be maintained at the concentration level of 11.3921 mg L⁻¹ and at the time of 47.35 min.

Keywords: Methyl orange dye; *Acalypha indica*; Isotherm; Breakthrough curve; Gravitational search algorithm

1. Introduction

The modern era of development of technologies has seen a tremendous increase in products leading to the destruction of our ecosystem. Water pollution is one of the serious concerns caused by the impact of these technological developments [1,2]. Dyes are one of the important factors contributing to water pollution. There are different categories of dyes like acidic dyes, basic dyes, reactive dyes, azo

dyes, etc. [3]. Production of dyes has increased due to their extensive use in textile industry [4]. There are a maximum of 0.7 million tonnes of synthetic dyes produced because of dyeing operations out of which 200,000–280,000 tonnes are released into the environment [5]. Dyes that are released into water bodies are hard to deteriorate, and due to their mutagenic nature, they have carcinogenic effects. Thus, controlling water contamination has turned into a critical issue in recent years [6,7]. The concentration of colored dyes has to be reduced to specific, tolerable limits before discharging them into water bodies. Wastewater generated from textile

* Corresponding author.

industry is evaluated based on the ejection volume and ignition of effluent. Therefore, an appropriate and cost-effective dye removal technology has to be developed to treat the effluent [8]. To treat these effluents, some chemical and physical methods that include coagulation, oxidation, absorption, filtration, ionization, radiation, etc. are employed [9,10]. These techniques pave the way for the creation of secondary pollutants (sludge) which needs to be treated further. Commonly available natural adsorbents having low cost, ready availability, capacity to create less sludge, and environmental friendly are considered to be the best options [11]. At present, the process of adsorption is one of the most efficient and attractive processes for the remediation of textile dyes [12]. Activated carbon is a promising adsorbent though it has a few demerits like high operating expenses and problems in recovering the spent carbon.

Utilization of naturally available materials as adsorbents for the treatment of wastewater would give us a potential substitute to the customary treatment strategies. Therefore, natural and squander materials from industry and farming can be utilized as alternative adsorbents [13]. These adsorbents are evaluated based on cost, availability, adsorption capacity, and their functional groups on the surface. They have unique surface functional groups like amino, phosphate, carboxyl, and the lipid division which are essential for adsorption. Biosorbents derived from apple pomace, wheat straw, coconut shell, coir pith, corncobs, barley husks, bentonite clay, fly ash, etc. have been found to be more effective than commercial activated carbon [14–19]. Among the different biosorbents known to us, biomass derived from Neem tree, *Acalypha indica* (Meliaceae), is highly potential and has been widely explored for solving various problems related to agriculture, public health, and environmental pollution control. Neem tree is native to Southeast Asia and grows in many countries throughout the world for the production and commercialization of various products. Their biomasses are used commonly for removal of toxic pollutants such as dye, pesticides, heavy metals, hydrocarbons, chemicals, radioactive compounds, etc. [20]. Biomass made from *A. indica* leaf serves as a potential alternative adsorbent since the surface structure remains stable even after longtime agitation treatment and also can be obtained without excessive cost highlighting its advantage as adsorbents. Treatment of dyes was carried out in batch mode but in order to obtain the results for industrial scale, column operation is preferable [21]. In addition, packed columns are found to be efficient since the flow of adsorbate is continuous which increases the adsorption capacity [22]. The application of classical optimization techniques is inevitable in modern process industries to increase the productivity and to obtain the maximum benefit out of it. The conventional optimization technique can address the problem if the dimensional space is less. If the intensity of the problem increases exponentially, the conventional optimizing techniques will not fulfill the requirement. Currently, Gravitational search algorithm (GSA), an optimization tool, is effectively utilized to overcome the aforementioned problems [23].

The objective of the current study is to reveal the potentiality of *A. indica* leaf as a suitable biosorbent for the removal of methyl orange dye. With respect to this, studies have been carried out in batch to find the effect of various operating

parameters like adsorbent dosage, pH of dye solution, and adsorption time. Langmuir, Freundlich, and Henry's models are utilized to evaluate the equilibrium data. The data gained from kinetic study are used to analyze pseudo-first-order, pseudo-second-order, intraparticle diffusion, and Elovich's models. Moreover, fixed-bed column studies were done to determine the performance of biomass in continuous operation in terms of breakthrough curve. As a part of this study, effects of bed depth, flow rate, and initial feed concentration on the performance of adsorption were also investigated. Further, to evaluate the breakthrough results, Thomas model was applied to the experimental data. And also, GSA tool is effectively utilized for optimization.

2. Materials and methods

2.1. Materials

Methyl orange dye with a purity of 99.9% was purchased from Balaji Chemicals Ltd., Chennai, India, to be used in the investigation. The dye stock solution ($1,000 \text{ mg L}^{-1}$) was prepared by dissolving a (1 g L^{-1}) known amount of methyl orange dye in distilled water. The experimental solutions were acquired by diluting the stock solutions with distilled water to preferred concentration. Analytical grade chemicals and reagents used in this study were purchased from Merck, Mumbai, India. They were used nascent without any further purification.

A. indica leaves were collected from the campus of Kalasalingam Academy of Research and Education, Tamil Nadu, India. They were rinsed with tap water followed by distilled water to get rid of dust particles and further dried in hot air oven at 70°C for 48 h. The dried leaves were powdered in laboratory mixer, and the particles were passed through a British Standard Sieve (BSS) of 44 mesh (350μ) and retained in 60 mesh (250μ), which were then collected and stored in poly bags for further study.

2.2. Characterization of biosorbent

Scanning electron microscopy (SEM) S-3000H (Hitachi, Japan) was used to determine the surface morphology, and the surface functionality of the biosorbent was identified by Fourier transform infrared (FTIR). The FTIR spectrum of the biomass before and after dye adsorption was recorded using an RTracer-100, FTIR spectrophotometer (Shimadzu, Japan). They were analyzed under constant conditions in the region from 400 to $4,000 \text{ cm}^{-1}$. Surface area of biosorbent was determined by Quanta chrome Autosorb 1C BET Surface Area & Pore Volume Analyzer (Quantachrome Instruments, USA).

Boehm titration was adapted to quantify the oxygen-containing surface functional groups [24]. For this titration, 0.1 N of NaOH, sodium carbonate, sodium bicarbonate, and hydrochloric acid were prepared as a stock solution separately. One gram of biomass was mixed with 50 mL of each stock solution in 5 different vials and shaken for 24 h. Then it was filtered, and from the filtrate, 5 mL was taken and titrated against the stock solution. During the titration, carboxylic acid was neutralized by sodium bicarbonate; carboxylic acid and lactonic groups were neutralized by sodium carbonate;

Carboxylic acid, lactonic and phenolic groups were neutralized by sodium hydroxide. Based on these assumptions, acidic sites were quantified.

The point of zero charge (pH_{pzc}) is the key factor that determines the type of surface active centers and the adsorption capacity of the chosen biosorbent [25]. Therefore, influence of pH on adsorption process plays a vital role. In order to find out pH_{pzc} powder addition method was selected in which 0.02 g of biosorbent was added to 20 mL of 0.1 M NaCl. The pH of the solution was adjusted from 2 to 11 using 0.1 M HCl or 0.1 M NaOH. This solution was equilibrated for 24 h after which the final pH of the solution was recorded (pH_f). Graph is plotted between ΔpH (i.e. difference between initial (pH_i) and final pH (pH_f)) and initial pH (pH_i).

2.3. Batch studies

Batch biosorption experiments were carried out in 100 mL of dye solution in an Erlenmeyer flask of 250 mL. Biomass from *A. indica* leaves was used as an adsorbent. To study the effect of sorbent dosage, different weights (0.01, 0.02, 0.03, 0.04, and 0.05 g) were measured and added to dye solution. The flasks were agitated on a shaker at 180 rpm with an initial dye concentration of 30 mg L^{-1} till the equilibrium was reached. Effect of pH on dye adsorption was studied at different pH (1, 2, 3, 4, 5, and 6 pH), where the solution pH was adjusted by adding 0.1 M NaOH or HCl solution. The adsorbent dose and dye concentration were set at optimum dose and 30 mg L^{-1} respectively. The influence of contact time was studied from 0 to 195 min with a time interval of 15 min under the identical parameters along with the optimized pH. All the experiments were conducted at 30°C.

A sample of 2 mL was withdrawn at different time intervals from the flask. It was centrifuged at 3,000 rpm for 3 min, and the supernatant liquid was analyzed for residual dye concentration. The absorbances of solution were studied at a maximum wavelength (λ_{max}) of 520 nm in UV-2700 UV-Vis spectrophotometer (Shimadzu, Japan). The amount of dye adsorbed per adsorbent mass was calculated by using the following equations:

$$q_t = \frac{(C_0 - C_t)V}{W} \quad (1)$$

$$q_e = \frac{(C_0 - C_e)V}{W} \quad (2)$$

where q_t and q_e are the amount of dye adsorbed (mg g^{-1}) at time t (mins) and at equilibrium time (min), respectively. C_0 , C_t and C_e represent the dye concentrations of methyl orange (mg L^{-1}) at zero time, at any time t , and at equilibrium time in the solution, respectively. V is the volume of solution (L), and W is the mass of adsorbent (g).

To ascertain the purpose of reproducibility of reported results, triplicate experiments were conducted and their standard deviations taken for further investigations [26]. This is indicated by error bars representing the standard deviation of a data set which are incorporated in the figures.

2.4. Equilibrium modeling in batch system

The behavior and the mechanism of the sorption of methyl orange onto *A. indica* were studied through equilibrium modelling. As defined by the isotherms, the amount of adsorbate adsorbed by the adsorbent as a function of its concentration was used. The adsorption data were analyzed using three isotherm models, namely, Langmuir, Freundlich, and Henry's models, for the present investigation.

2.4.1. Langmuir model

The Langmuir adsorption model is the most common one used to quantify the amount of adsorbate adsorbed on an adsorbent. Langmuir model assumes that adsorption is monolayer, and it may be due to physisorption which involves weak intermolecular forces such as Van-der-Waals force of attraction and hydrogen bonding. It can be described by Eq. (3).

$$\frac{C_e}{q_e} = \frac{1}{bQ_0} + \frac{C_e}{Q_0} \quad (3)$$

where C_e is the equilibrium concentration of dye (mg L^{-1}), q_e is the amount of dye adsorbed onto biosorbent at equilibrium time (mg g^{-1}), Q_0 and b are the maximum amount of the dye per unit weight of biomass to form a complete monolayer on the surface bound at high q_e , and b is a constant related to the affinity of the binding sites, respectively.

According to Eq. (3), a plot of C_e/q_e versus C_e will be a straight line with a slope $1/Q_0$ and intercept $1/bQ_0$ when adsorption follows the Langmuir equation.

2.4.2. Freundlich model

The Freundlich model explains the multilayer adsorption. It is an empirical relation between the concentration of a solute on the surface of an adsorbent and the concentration of the solute in the liquid with which it is in contact. It is believed to happen due to chemisorption which involves formation of strong chemical bonds. It is irreversible, and it requires high activation energy. The following equation represents the Freundlich isotherm.

$$\ln q_e = \ln K + \frac{1}{n} \ln C_e \quad (4)$$

where K and n are adsorption capacity (mg g^{-1}) and adsorption intensity, respectively. Eq. (4) can be linearized, and the graph was plotted between $\ln q_e$ and $\ln C_e$ to determine Freundlich constants. The magnitude of the term $(1/n)$ gives an indication of the favorability of the sorbent-adsorbate systems.

2.4.3. Henry's isotherm

Henry's law is applied to the system where the adsorption is carried out on a uniform surface at sufficiently low concentrations such that all molecules are eliminated from their neighbors. The relationship between fluid phase and

adsorbed solid phase are in equilibrium and was found to be linear with a constant of proportionality known as the Henry's constant (k_H). The following equation represents the Henry's isotherm.

$$\ln q_e = \ln k_H + \ln C_e \quad (5)$$

Graph was plotted between $\ln q_e$ and $\ln C_e$ to determine Henry's constant (k_H)

2.5. Kinetic modeling in batch system

In order to investigate the mechanism of biosorption and potential rate controlling steps such as mass transport, chemical reaction processes, and kinetic models play a major role to test the experimental data. When the biomass is suspended in a well-agitated batch system, all the binding sites present on the wall are made readily available for dye uptake so that the effect of diffusion on biosorption rate can be assumed to be insignificant and hence omitted from the analysis. The kinetic models including the pseudo-first-order, pseudo-second-order, intraparticle diffusion, and Elovich's models can be used in this case assuming that the measured concentrations are equal to surface concentrations.

2.5.1. Pseudo-first order

Pseudo-first-order rate expression is specified by Eq. (6)

$$\log(q_e - q_t) = \log q_e - \frac{k_1 t}{2.303} \quad (6)$$

where q_e is the adsorption capacity at equilibrium (mg g^{-1}), q_t is the adsorption capacity of sorbent at any time (mg g^{-1}), and k_1 is the pseudo-first-order rate constant (min^{-1}). Plot was made between $\log(q_e - q_t)$ and t was made to find the constant k_1 .

2.5.2. Pseudo-second order

Pseudo-second-order rate expression is given by Eq. (7).

$$\frac{t}{q_t} = \frac{1}{k_2 q_e^2} + \frac{t}{q_e} \quad (7)$$

where q_e is the adsorption capacity at equilibrium (mg g^{-1}), q_t is the adsorption capacity at any time (mg g^{-1}), and k_2 is the pseudo-second-order rate constant ($\text{g mg}^{-1} \text{min}^{-1}$). Values of q_e and k_2 can be calculated by plotting t/q_t and t .

2.5.3. Intraparticle diffusion model

In intraparticle diffusion model, the medium possesses a uniform concentration of sites on which the solute molecules form a monolayer. Based on the previous results on the kinetic behavior of biosorbent, intraparticle diffusion was found to be the most significant factor in the adsorption process [27]. Hence, the possibility of diffusion of adsorbate species into adsorbent affecting adsorption was estimated

by this model. Rate expression for the above said model is represented in Eq. (8).

$$q_t = k_p t^{1/2} + C \quad (8)$$

where q_t is the amount of dye adsorbed at time t (mg g^{-1}), C is the intercept, and K_p is the intraparticle diffusion rate constant ($\text{mg g}^{-1} \text{min}^{1/2}$). K_p values were obtained from the slope of the straight line portions of plot made between q_t and $t^{1/2}$.

2.5.4. Elovich's model

The Elovich equation has been widely used in adsorption kinetics, which describes chemical adsorption mechanism in nature. The approaching equilibrium parameter of Elovich equation was used here to describe the characteristic curves of adsorption kinetics. It is suitable for the system whose adsorbing surfaces are heterogeneous. Elovich's equation is stated as:

$$q_t = \frac{1}{b} \ln(ab) + \frac{1}{b} \ln t \quad (9)$$

where a is initial rate of adsorption ($\text{mg g}^{-1} \text{min}$) and b is Elovich's constant that signifies the intensity of adsorption (g mg^{-1}).

2.6. Column studies

Continuous studies were performed using a column made of glass with a diameter and length of 1.5 and 15 cm, respectively. A known amount of *A. indica* biomass was packed in the column to a preferred bed height. Two sieves and a layer of glass beads were placed at the top and bottom of the column to prevent the entrainment of biomass and to distribute and maintain uniform flow of the solution. Dye solution was fed from the bottom to the top of the column with the help of peristaltic pump (Watson-Marlow 323E). The column was operated at different bed heights of 3, 6, and 9 cm and flow rates of 5, 10, and 15 mL min^{-1} at a constant pH. The concentration of methyl orange at the exit of the column was analyzed at predefined time intervals. The breakthrough curves were obtained by plotting the ratio C/C_0 of methyl orange dye concentration vs. time, where C_0 is the concentration of dye at zero time (mg L^{-1}) and C is the concentration of dye at any time t (mg L^{-1}).

2.6.1. Equilibrium modeling in continuous system

The adsorption data of column experiments were evaluated by Thomas model. The main advantage of using this model is its effortlessness and exactness in anticipating the saturation capacity. The modelling equation is given below:

$$\frac{C}{C_0} = \frac{1}{1 + \exp(K_T [q_0 m - C_0 V] / Q)} \quad (10)$$

where K_T is the Thomas rate constant ($\text{mL min}^{-1} \text{mg}^{-1}$) and Q is the volumetric flow rate of methyl orange dye (mL min^{-1}).

The linearized form of Thomas model is given by Eq. (11).

$$\ln\left(\frac{C_0}{C} - 1\right) = \frac{K_T q_0}{Q} - \frac{K_T C_0}{Q} V \quad (11)$$

The kinetic coefficient K_T and the sorption capacity of the bed q_0 can be calculated by plotting $\ln(C_0/C - 1)$ and time at a specified flow rate.

2.6.2. GSA optimization

The classical optimization algorithms are most suitable for solving problems with small dimensional space, and if the intensity of the problem increases exponentially, it leads to exhaustive search. Exhaustive search is not possible by the conventional algorithm. Recently, many algorithms have been developed based on the inspiration of natural phenomena. Among them, GSA is applied rarely in adsorption domain. In this work, an attempt has been made to apply these algorithms, one based on animal behavior and the other on the law of gravity. Both these algorithms are inspired by nature, but the source of natural phenomena is entirely different.

The law of Newtonian gravity states that the force of attraction between two things is directly proportional to the product of their masses and inversely proportional to the square of the distance between them. It can be mathematically expressed as in Eq. (12).

$$F = G \frac{m_1 m_2}{d^2} \quad (12)$$

where G is the gravitational constant, m_1 and m_2 are mass of the particles 1 and 2 respectively, d^2 is the distance between the particles, and F is the force acting between the particles.

The Newton's second law of motion describes the relationship between force and acceleration as shown in Eq. (13).

$$F = m \times a \quad (13)$$

where a is the acceleration due to gravity.

Based on Eqs. (12) and (13), it is understood that the size of the mass is bigger and the force of attraction is also higher. The force of attraction is higher than the acceleration due to gravity. In Eq. (12), G represents gravitational constant, and the gravitational constant value depends on the age of the universe. As the age of the universe increases, the gravitational constant G value decreases. The decrease in G value can be computed by Eq. (14).

$$G(t) = G(t_f) \left(\frac{t_f}{t}\right)^\beta \quad (14)$$

where $\beta < 1$, $G(t)$ represents the gravitational constant value at time t and $G(t_f)$ represents the gravitational constant value

at the first cosmic interval time t_f . Eqs. (12) and (13) can be precisely written as

$$F_{ij} = G \frac{m_{ai} m_{pj}}{d^2} \quad (15)$$

$$a_i = \frac{F_{ij}}{m_{ii}} \quad (16)$$

As per theoretical physics, mass can be classified into three categories, namely, active, passive, and inertial mass. Active mass is the measure of strength of the gravitational field of the particular object. The strength of the active gravitational field increases in relation to objects and vice versa. Passive mass is the measure of the gravitational field due to the interaction between the particles. Interaction between the particles leads to higher gravitational field. In case of inertial mass, it resists the acceleration of the object if the mass is higher than the effect of resistance as described in Eq. (16). In Eqs. (15) and (16), m_{ai} , m_{pj} and m_{ii} represent the active, passive, and inertial mass of the particle, where F_{ij} is the force acting on mass i by mass j . In this algorithm, particles are considered as adsorbent and their performance is measured by masses. Each mass has certain specifications which are position, active, passive, and inertial gravitational mass. The position of the algorithm helps us to find the optimum solution, whereas fitness function is derived from the active, passive, and gravitational mass. A dimensional space with N number of agents is taken to find the position of the optimum agent say i^{th} agent, and it can be defined as

$$X_i = (X_i^1, \dots, X_i^d, \dots, X_i^n) \quad \text{for } i = 1, 2, 3, \dots, N \quad (17)$$

where X_i^1 presents the position of the i^{th} agent in the d^{th} space. Force acting on m_{ai} and m_{pj} can be defined as

$$F_{ij}^d(t) = G(t) \frac{M_{pi}(t) M_{aj}(t)}{R_{ij}(t) + \epsilon} (X_j^d(t) - X_i^d(t)) \quad (18)$$

The euclidean distance between the objects can be determined by the following expression:

$$R_{ij}(t) = \|X_i(t), X_j(t)\| \quad (19)$$

Force acting on mass (agent) i is determined by giving random weightage to the force acting on mass i by j in the dimensional space (d_i).

$$F_i^d = \sum_{j=1, j \neq i}^N \text{rand}_j F_{ij}^d \quad (20)$$

The random number is in the interval of 0 to 1. Therefore, force calculation of the agent i at time t can be given as

$$a_i^d = \frac{F_i^d}{M_i^d} \quad (21)$$

The change in the position of the agent with respect to time can be defined by velocity or acceleration, and the velocity or acceleration at a specific time can be represented as the sum of fraction of its previous velocity and variation in the velocity. The velocity at a specific time is

$$V_i(t+1) = \text{rand}_i V_i^d + a_i^d(t) \quad (22)$$

$$X_i^d(t+1) = X_i^d(t) + V_i^d(t+1) \quad (23)$$

The gravitational constant depends on the age of the universe. Therefore, the initial gravitational constant is initialized in the beginning, and it varies and reduces with respect to time. Hence, G depends on G_0 and t .

$$G(t) = G(G_0, t) \quad (24)$$

The inertial mass and gravitational mass are calculated by fitness evaluation, and the calculated values are updated by Eq. (25). Therefore, Eq. (20) can be modified as:

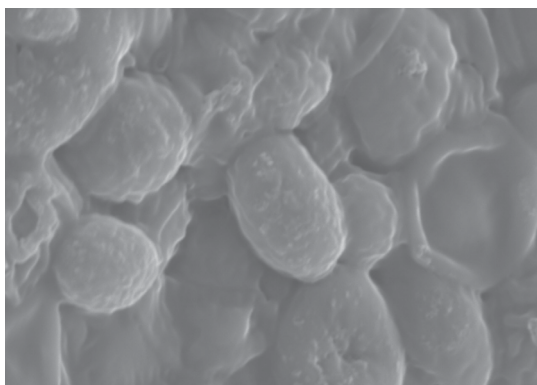
$$F_i^d = \sum_{j \in k \text{ best } j \neq i} \text{rand}_j F_{ij}^d \quad (25)$$

3. Results and discussion

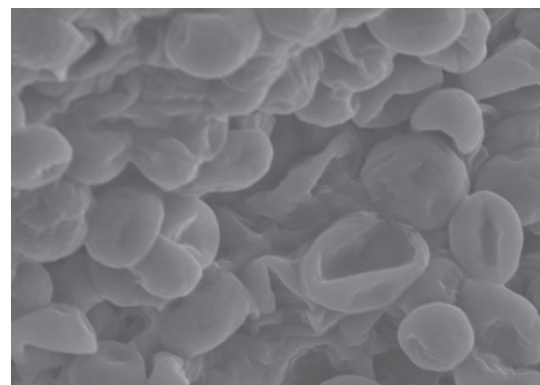
3.1. Biosorbent characterization

3.1.1. SEM analysis

Fig. 1 shows the SEM image of *A. indica* biomass before and after adsorption of methyl orange dye solutions with a concentration of 30 mg L⁻¹. In this image, bigger particles of irregular spherical clusters with rough and curly surfaces were found on the surface of biosorbent which increases the contact area for the adsorption between the biosorbent and adsorbate. Figs. 1(a) and (b) illustrate the surface morphology of the sorbent before and after the sorption. As stated above, before the sorption process, the surface morphology of biomass possesses rough surface. While after adsorption of dye on to biomass, surface of biosorbent was found to be smoother throughout.



(a) Before adsorption



(b) After adsorption

Fig. 1. SEM images of *A. indica* biomass.

3.1.2. FTIR analysis

Surface oxygen groups enhance the dye adsorption. Fig. 2 shows that the presence of such groups indicated by the absorption bands at 3,430, 2,630, 1,637, and 1,070 cm⁻¹ which represent the presence of -OH, C=O, C=C, and C-O stretching vibrations, respectively. The peak position at 3,390 cm⁻¹ has become less intense and has shifted to 3,433 cm⁻¹ after adsorption. This region has been assigned to O-H stretching groups which interact with methyl orange dye. There is a disappearance of peaks in the regions of 2,364 and 2,345 cm⁻¹ in FTIR spectrum of biosorbent after dye adsorption which is due to the change of hydroxide group into C=C=C or C=C=O during adsorption of anionic dye. The bands at 1,538 cm⁻¹ are attributed to NH scissoring vibrations which after adsorption appears at 1,524 cm⁻¹ thereby providing NH groups which are also responsible for adsorption. The C=O stretching of the ketonic group at 1,732 cm⁻¹ is absent after adsorption and instead a new peak appears at 1,714 cm⁻¹ due to C=O stretching of the carboxylic group. The significant decrease in the intensity of most of the groups reveals the possible participation of these groups in the adsorption of methyl orange on the whole. These results are in agreement with the works reported in literature [28].

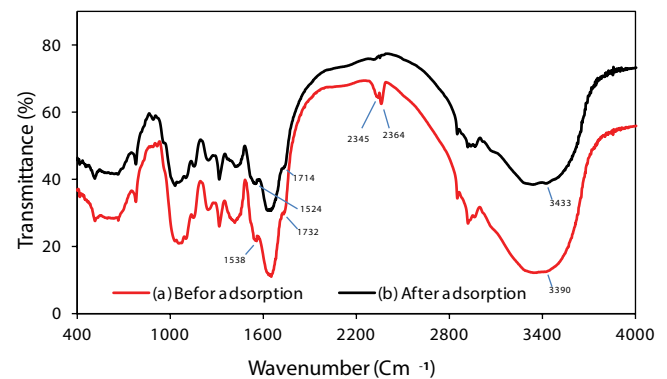


Fig. 2. FTIR spectrum of *A. indica* biomass before and after methyl orange adsorption.

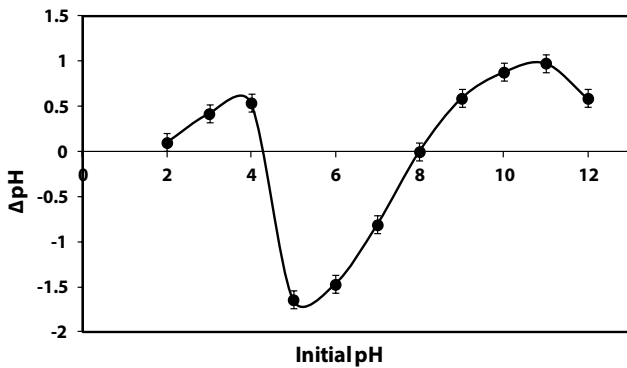


Fig. 3. Point of zero charge of *A. indica* biomass.

3.1.3. Boehm titration

Neutralized values of carboxylic, lactonic, phenolic, and basic groups were found to be 0.421, 0.078, 0.000, and 0.166 mol m⁻², respectively. The total strength of acid sites is found to be 0.499 mol m⁻². Hence, the charge on the surface was found to be acidic [29]. This result is supported by point of zero charge analysis.

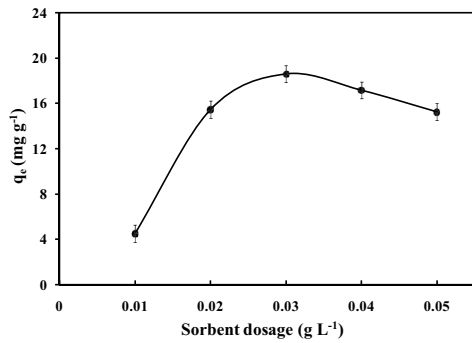
3.1.4. Point of zero charge (pH_{pzc})

To determine the charge on the surface of the biomass, graph is plotted between ΔpH (pH_i - pH_p) and initial pH (pH_i).

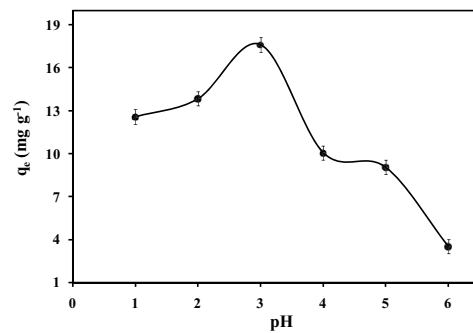
From Fig. 3, it is clear that anionic dye adsorption is favorable (pH < pH_{pzc}) due to the presence of positively charged particles on the surface of the adsorbent. It is observed that the pH between 1 and 3 leading to an increase in the uptake capacity of biosorbent is high after which it begins to decrease. This may be due to the fact that negatively charged ions in the dye solution are attracted toward the electrostatic force of positively charged ions present on the surface of the biosorbent. Hence, anionic dye (methyl orange dye) adsorption takes place at lower pH. Therefore, absorption of methyl orange dye by *A. indica* biomass is favorable at lower pH. A similar tendency has been recorded in the literature by Jirekar et al. (2014) for the adsorption of methylene blue dye onto the surface of *Phaseolus aureus* [18].

3.2. Effect of biosorbent dosage

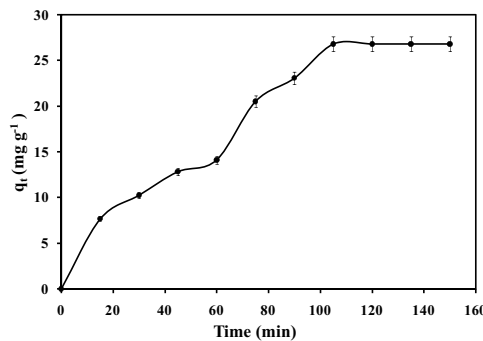
It is inferred from Fig. 4(a) that the uptake capacity of sorbent increases from 4 to 18 mg g⁻¹ as the sorbent dosage is increased from 0.01 to 0.03 g, respectively. This phenomenon is due to the availability of vast number of adsorption sites and huge surface area of biosorbent that makes the penetration of dye to the adsorption site easier. At 0.03 g, the biomass shows maximum uptake capacity where it reaches the equilibrium. But above 0.03 g, uptake capacity starts to decrease because the adsorptive capacity of the adsorbent available is not fully utilized at a higher adsorbent dosage in comparison with lower adsorbent dosage due to the saturation of adsorption sites and agglomeration of biomass. Therefore,



(a) Effect of sorbent dosage at 150 min



(b) Effect of pH at 150 min



(c) Effect of contact time

Fig. 4. Effect of various parameters on the uptake capacity for the adsorption of methyl orange dye onto *A. indica* (temperature = 30°C; agitation rate = 180 rpm; adsorbent dose = 0.03 g; dye concentration = 30 mg L⁻¹).

it might be possible that adsorption capacity decreases as adsorbent dosage increases [30].

3.3. Effect of pH

Fig. 4(b) shows that when pH is increased toward 3, the uptake capacity of the sorbent also increases because the pH of the dye solution is highly dependent on ionization resulting in strong electrostatic force of attraction between anionic dye molecules and cationic sorbent. But after pH 3, it begins to decrease due to the increase in the formation of nonionic surface functional groups that reduce the dye uptake capacity. Therefore, pH 3 was selected for equilibrium and kinetics studies. This phenomenon is in accordance with the result obtained in point of zero charge analysis. Literature survey shows a similar behavior of adsorption of Pb(II) ions on maize tassel [31].

3.4. Effect of contact time

The contact time between dye and sorbent plays an important role in the adsorption process [32]. From Fig. 4(c), it is clear that when time increases, uptake capacity also increases. This is due to the fact that the active sites present on the surface of the sorbent are sufficient enough to adsorb the dye. But when the contact time is increased,

the adsorption site, as well as the driving force between the sorbent and the dye ions, decreases, and it reaches the equilibrium at 150 min. When the contact time is increased beyond 150 min, the active sites get saturated and adsorption remains constant.

3.5. Adsorption isotherms

A linear plot made between C_e/q_e and C_e for Langmuir isotherm and $\ln q_e$ and $\ln C_e$ for Freundlich and Henry's isotherms are shown in Figs. 5(a)–(c), respectively. The corresponding values of regression factor and correlation coefficients are represented in Table 1. From the isotherm plots, it is clear that the experimental data fit well with Henry's isotherm ($R^2 = 0.997$) than that of Langmuir isotherm ($R^2 = 0.813$) and Freundlich isotherm ($R^2 = 0.9772$). The estimated k_H value demonstrates the liking among the adsorbate and the adsorbent, thereby making the adsorption multi-layer. The adsorption intensity k_H is found to be 2.1728, and the analogous results of $R^2 > 0.99$ and $k_H > 1$ are in accordance with the results discussed in literature [33].

3.6. Biosorption kinetics

Kinetics of adsorption of methyl orange dye onto biosorbent were analyzed using pseudo-first-order, pseudo-second-

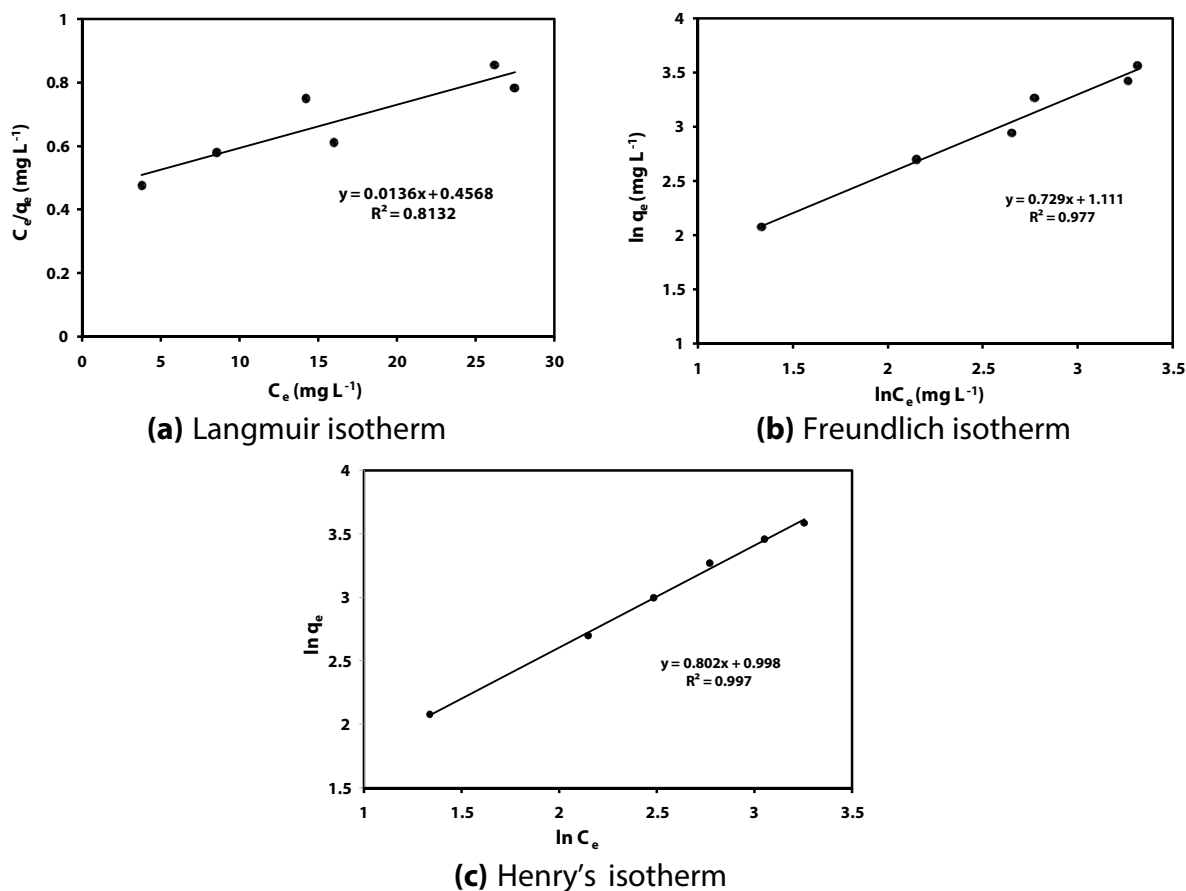


Fig. 5. Adsorption isotherms.

Table 1
Langmuir and Freundlich isotherm constants

Langmuir constant			Freundlich constants			Henry's constant	
q_{\max} (mg g ⁻¹)	b_L (L mg ⁻¹)	R^2	$1/n$	K_f (L g ⁻¹)	R^2	k_H (L g ⁻¹)	R^2
76	0.02	0.813	0.7290	3.0373	0.977	2.7128	0.997

order, intraparticle diffusion, and Elovich's models. A linear plot obtained for the applicability of these models is shown in Fig. 6. The value of regression factor and correlation coefficients are represented in Tables 2 and 3 that show the comparative analyses for biosorption rate constants. It was found that the Elovich's model is better when compared with the other three models. This is justified from the values of regression coefficient (R^2 values) represented in Table 2 having values greater than 0.99. In addition to this, the values of the experimental and calculated uptake capacity (q_e) were approximately similar for this model. Hence, from the above investigation, it is proved that the biosorption of methyl orange by *A. indica* obeys the Elovich's model. Comparable outcomes have been accounted in literature for biosorption process [34].

3.7. Column studies

As shown in Fig. 7, the breakthrough curves were obtained by plotting the ratio (C/C_0) of methyl orange dye concentration vs. time (t) where C_0 is the concentration of methyl orange dye at zero time (mg L⁻¹) and C is the concentration of methyl orange dye solution at any time t (mg L⁻¹).

3.7.1. Effect of bed height and flow rate

Continuous experiments were carried out in a column filled with *A. indica*, and the bed height was varied. The breakthrough and exhaustion time were calculated for the different bed heights at various flow rates. Both the breakthrough and exhaustion time were observed to expand with increase in bed height.

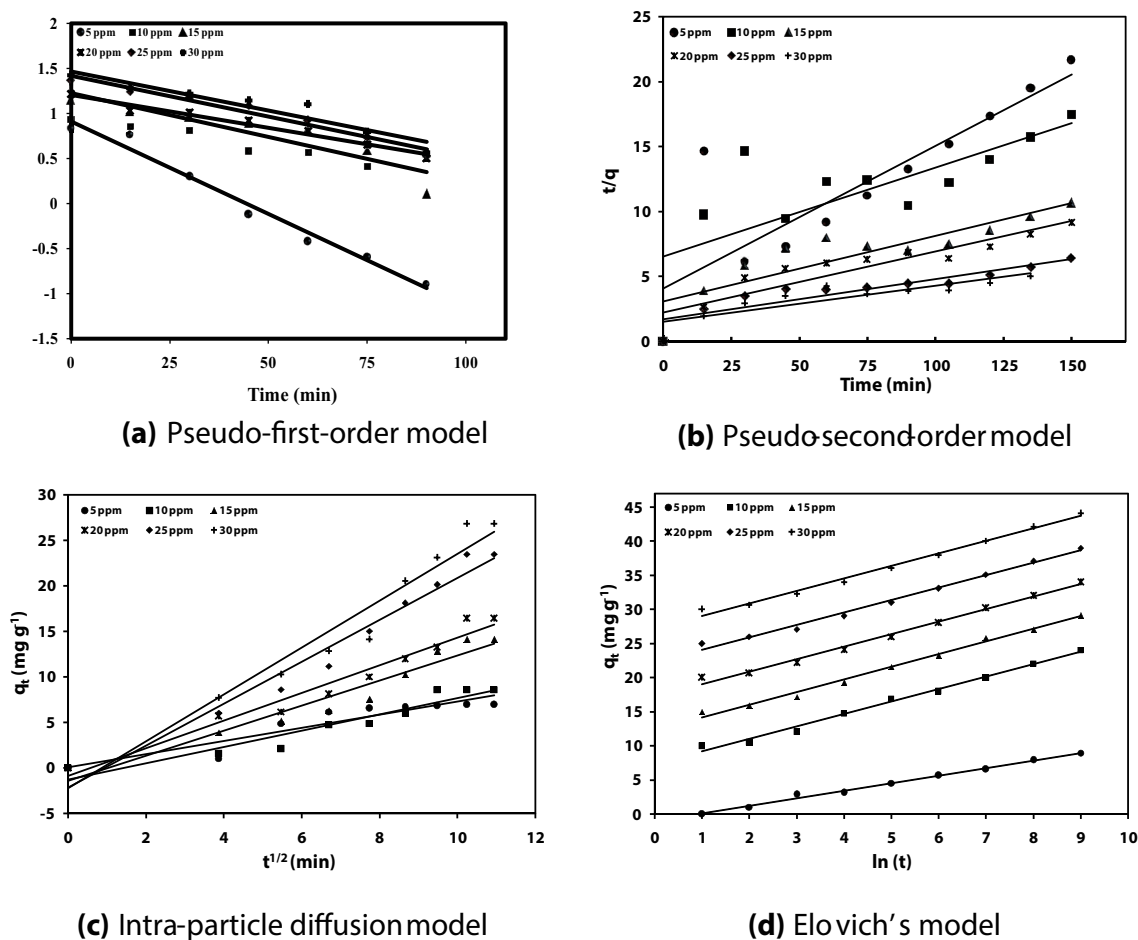


Fig. 6. Kinetic models.

Table 2
Kinetic parameters

Dye concentration (mg L ⁻¹)	q_e experimental value (mg g ⁻¹)	Pseudo-first-order model			Pseudo-second-order model			Elovich's model			
		q_e (mg g ⁻¹)	k_1 (min ⁻¹)	R^2	q_e (mg g ⁻¹)	k_2 (g mg ⁻¹ min ⁻¹)	R^2	q_e (mg g ⁻¹)	a (mg g ⁻¹ min)	b (g mg ⁻¹)	R^2
5	7.9615	8.18	0.01	0.979	1.174	0.04	0.738	7.5	12.5	0.9015	0.9938
10	14.3461	9.05	0.016	0.95	1.619	0.032	0.5478	13.65	16.72	0.9475	0.9911
15	18.9615	16.9	0.02	0.835	5.762	0.016	0.7638	15.7	25.30	0.8321	0.9914
20	26.0769	22.18	0.016	0.971	5.231	0.051	0.8405	21.07	32.51	0.8444	0.9913
25	30.6538	26.06	0.02	0.962	8.1543	0.0182	0.841	25.71	43.75	0.8491	0.9909
30	35.1538	29.44	0.018	0.908	11.23	0.018	0.7967	29.03	54.51	0.8715	0.9915

Table 3
Intraparticle diffusion model

Dye Concentration (mg L ⁻¹)	K_p (mg g ⁻¹ min ^{1/2})	C (mg g ⁻¹)	R^2
5	1.3751	1.2865	0.9010
10	1.5219	1.4151	0.9096
15	2.3013	2.1596	0.9393
20	2.5718	3.570	0.9624
25	3.2124	6.670	0.9657
30	3.7013	8.010	0.9494

In this study, the maximum obtainable level of methyl orange removal was analyzed by altering the flow rates of the sample at different bed heights. From Table 4, it is observed that if the bed height is increased, then the exhaustion time and breakthrough time also increase. This is because of the fact that the zone of mass transfer accessible for adsorption is enlarged and the quantum of binding sites is improved to make sorption easier. The column adsorption performed well at the least reduced flow rate than at higher flow rates. This happens because of inadequate contact time of solute and adsorbent inside the column and the dissemination confinements of the solute into the pores of the adsorbent

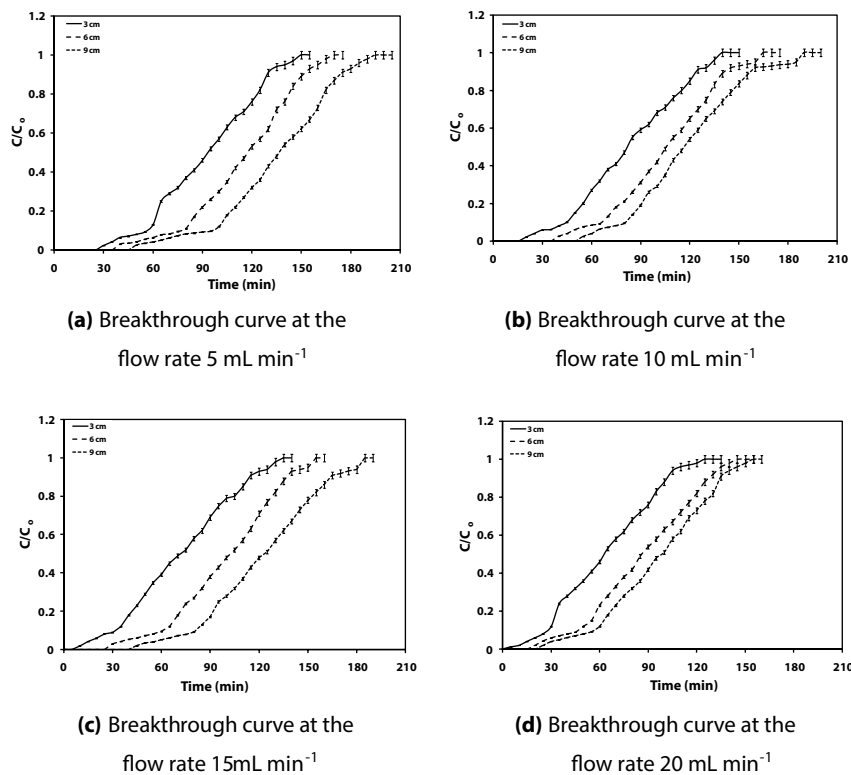


Fig. 7. Breakthrough curves for biosorption of methyl orange dye onto *A. indica* at various bed heights for the dye concentration 10 mg L⁻¹.

Table 4
Effect of different bed heights and various flow rates of 10 mg L⁻¹ methyl orange concentrations in column study

Bed height (cm)	Flow rate (mL ⁻¹ min)	Breakthrough time (min)	Exhaustion time (min)	Saturation capacity (mg g ⁻¹)
3	5	30	150	65.82
6	5	40	175	48.13
9	5	50	195	32.63
3	10	20	140	59.21
6	10	40	165	45.13
9	10	55	190	30.01
3	15	10	135	58.31
6	15	30	155	44.15
9	15	45	185	29.71
3	20	5	125	55.12
6	20	20	145	36.10
9	20	25	155	25.12

at higher flow rates. Additionally, the take-up limit of dye diminishes with increase in flow rate. A similar behavior is also reported in the adsorption of cephalixin by walnut shell-based activated carbon by Nazari et al. [35].

3.7.2. Effect of concentration

The biosorption capacity of *A. indica* on aqueous methyl orange dye was performed at various influent concentrations. The breakthrough curves were acquired by varying methyl orange concentration from 10 to 30 mg L⁻¹ as shown in Fig. 8. As a result of a decrease in influent methyl orange concentration, it leads to extended breakthrough curves. Since concentration gradient among the solute molecules was less, slow transport through the pores of adsorbent was promoted. At the highest concentration (30 mg L⁻¹), saturation of *A. indica* bed was quicker leading to early exhaustion time and breakthrough.

From Table 5, it was found that the maximum uptake was observed at the lowest bed height because of a decrease in

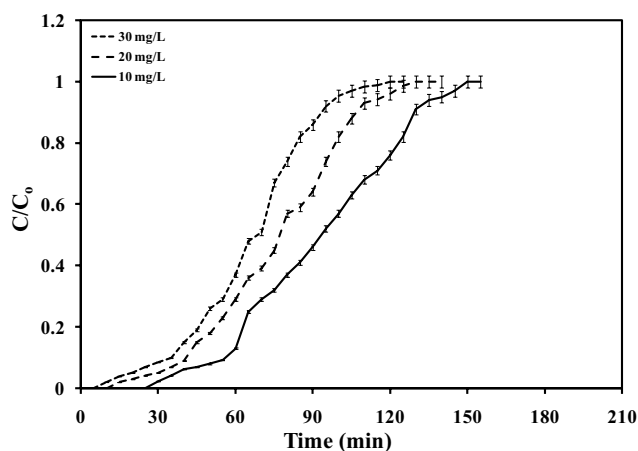


Fig. 8. Breakthrough curve at different concentrations of methyl orange dye onto *A. indica* at the flow rate of 5 mL min⁻¹ and bed height of 3 cm.

Table 5
Effect of concentration on optimum bed height (3 cm) and flow rate (5 mL min⁻¹)

Initial concentration (mg L ⁻¹)	Breakthrough time (min)	Exhaustion time (min)	Saturation capacity (mg g ⁻¹)
10	20	140	72.17
20	15	130	115.42
30	10	120	244.12

the quantity of adsorbent which offered more binding sites for adsorption. This shows that at smaller bed height, the effluent adsorbate concentration ratio increased more rapidly than for a higher bed height. Constructive breakthrough curve was obtained for 30 mg L⁻¹ methyl orange concentration. The driving force for adsorption is the concentration gradient between methyl orange on the adsorbent and in aqueous solution. Thus, higher concentration of methyl orange resulted in enhanced column performance. These outcomes are in good agreement with the results given in literature [35].

3.7.3. Modelling analysis of column data by the Thomas model

Fig. 9 shows a linear plot proving that the experimental data fit with the model for all flow rates with the regression coefficient (R^2) greater than 0.95. The Thomas equation coefficient for methyl orange dye adsorption is given in Table 6. From the table, it is observed that as the flow rate is increased, the value of K_T increases and the value of q_0 decreases. Identical performance was observed by Beheshti et al. in the removal of Cr (VI) from aqueous solutions using chitosan/multi-walled carbon nano tube (MWCNT)/Fe₃O₄ composite nanofibers [36].

3.7.4. Optimization of column study by GSA

The following process parameters are considered to optimize the equilibrium dye uptake limit of *A. indica*. Tables

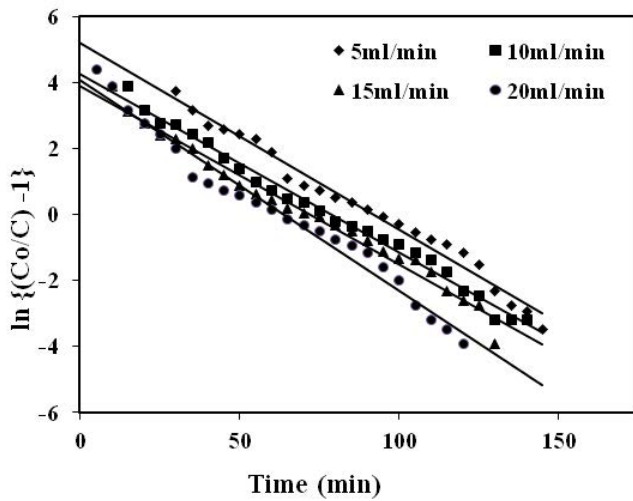


Fig. 9. Plot of $\ln((C_0/C) - 1)$ vs. time at different flow rates.

Table 6
Thomas model

Flow rate ($\text{mL}^{-1} \text{min}$)	K_T ($\text{mL min}^{-1} \text{mg}^{-1}$)	$q_{0, \text{cal}}$ (mg g^{-1})	$q_{0, \text{exp}}$ (mg g^{-1})	R^2
5	0.026	65.02	65.82	0.990
10	0.052	59.10	59.21	0.985
15	0.065	58.51	58.31	0.982
20	0.088	55.24	55.12	0.976

1–5 show the experimental result of batch and column studies. The result obtained during the experimentation is used to develop regression equation. Eq. (26) shows the dye equilibrium uptake limit model for the above mentioned process.

$$\text{EUTC} = (0.695 + 0.1173t - 0.234\text{IC} - 0.000733t^2 + 0.0075\text{IC}^2 + 0.005707t)\text{IC} \quad (26)$$

where EUTC is the equilibrium uptake capacity of the adsorbent and IC is the inlet concentration.

Since the objective of the experiment is to increase the dye uptake capacity, it is essential to determine the optimal values. The equation derived from regression equation is used as an objective function to determine the optimum values. The lower and upper limits of the process parameters are considered to be constrained. The constraints are $0 \leq \text{time} \leq 150$ and $5 \leq \text{uptake capacity} \leq 30$.

To determine the optimal solution for the aforementioned objective function and process parameters (constraints), the following procedure is followed. The selection of the suitable number among total number of agents, size of population, and initial value of gravitational constant is more important. Since this algorithm is not applied to solve the discussed problem, it is necessary to try numerous times to get consistency in results. The procedure is repeated one hundred times to check its consistency, and the average value is taken

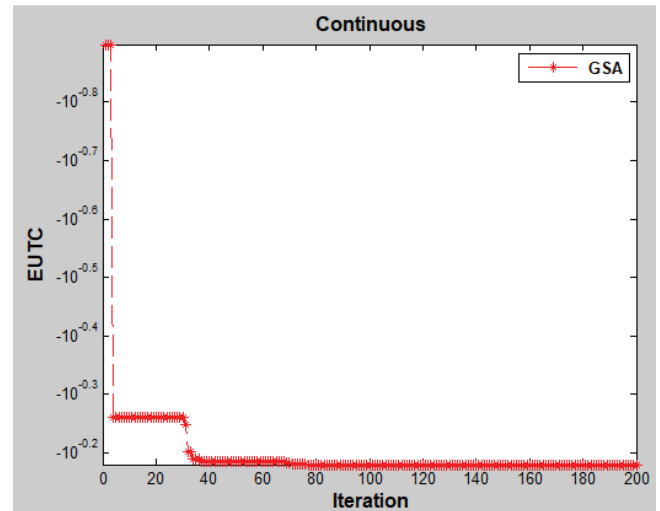


Fig. 10. Optimization of process parameters by GSA tool.

for deriving its optimal selection. Fig. 10 shows the GSA parameter used for identifying the optimal solution. It also describes the recommended optimal conditions for improving the dye uptake limit. It is observed that the optimum value for batch process is 35 mg g^{-1} and for column study is around 244 mg g^{-1} .

4. Conclusion

The current study examined the adsorption capacity of *A. indica* to remove methyl orange dye from an aqueous solution. The biomass was characterized for surface morphology, functional groups, and point of zero charge. Boehm titration was performed to determine the charge of biosorbent. Parameters influencing batch adsorption like adsorbent dosage, pH, and contact time were optimized. Point of zero charge of biosorbent was determined, and it was found to be around 8. The numbers of acid sites were found to be 0.499 mol m^{-2} . Biosorption kinetics studies demonstrated that the experimental data fitted exceptionally well with Elovich's model. Henry's isotherm was found to be a better fitting model than Langmuir and Freundlich isotherms. The utmost uptake capacity of biomass was found to be 76 mg g^{-1} at optimal pH of 3 and adsorbent dosage of $0.03 \text{ g } 100 \text{ mL}^{-1}$. Column studies indicated that the adsorption capacity (244 mg g^{-1}) of *A. indica* enhanced with increase in the preliminary influent concentration and diminished with bed height and flow rate. Column data were analyzed by Thomas model. In comparison with batch process, continuous process for adsorption of methyl orange dye from aqueous solution was found to be more efficient. Therefore, GSA was applied to continuous process experimental data, and it was found that the time of the process should be maintained at 47.35 min and the concentration level should be at $11.3921 \text{ mg L}^{-1}$.

Declaration

This research did not receive any specific grant from funding agencies in the public, commercial, or not-for-profit sectors.

References

- [1] H.N. Bhatti, J. Hayat, M. Iqbal, S. Noreen, S. Nawaz, Biocomposite application for the phosphate ions removal in aqueous medium, *J. Mater. Res. Technol.*, 7 (2018) 300–307.
- [2] L. Zhang, Y. Zeng, Z. Cheng, Removal of heavy metal ions using chitosan and modified chitosan: a review, *J. Mol. Liq.*, 214 (2016) 175–191.
- [3] A. Kausar, M. Iqbal, A. Javed, K. Aftab, H.N. Bhatti, S. Noreen, Dye adsorption using clay and modified clay: a review, *J. Mol. Liq.*, 265 (2018) 395–407.
- [4] A. Kanwal, H.N. Bhatti, M. Iqbal, S. Noreen, Basic dye adsorption onto clay/MnFe₂O₄ composite: a mechanistic study, *Water Environ. Res.*, 89 (2017) 301–311.
- [5] L.G.C. Villegas, S. Mazloum, K.E. Taylor, N. Biswas, Soyabean peroxidase-catalysed treatment of azo dyes with or without Feo pre-treatment, *Water Environ. Res.*, 90 (2018) 675–684.
- [6] X. Xu, M. Tian, L. Qu, S. Zhu, Graphene oxide/chitosan/polyvinyl-alcohol composite sponge as effective adsorbent for dyes, *Water Environ. Res.*, 89 (2017) 555–563.
- [7] P. Saravanan, P. Sivakumar, G. Geoprincy, G.N. Nagendra, S. Renganathan, Biosorption of acid green 1 using dried *Rhodotorula glutinis* biomass, *Indian J. Environ. Prot.*, 32 (2012) 207–214.
- [8] J. Lopez-Cervantes, D.I. Sanchez-Machado, R.G. Sanchez-Duarte, M.A. Correa-Murrieta, Study of a fixed-bed column in the adsorption of an azo dye from an aqueous medium using a chitosan-glutaraldehyde biosorbent, *Adsorpt. Sci. Technol.*, 36 (2018) 215–232.
- [9] D.D. Long, Q. Wang, J.R. Han, Biosorption of Copper (II) from aqueous solutions by sclerotogenic *Aspergillus oryzae* G15, *Water Environ. Res.*, 89 (2017) 703–713.
- [10] P. Saravanan, P. Sivakumar, T. Suganya, N.N. Gandhi, S. Renganathan, Bioaccumulation of reactive red 11 using live yeast *Rhodotorula glutinis*, *Indian J. Environ. Prot.*, 32 (2012) 249–255.
- [11] A.S. Sartape, A.M. Mandhare, V.V. Jadhav, P.D. Raut, M.A. Anuse, S.S. Kolekar, Removal of malachite green dye from aqueous solution with adsorption technique using *Limonia acidissima* (wood apple) shell as low cost adsorbent, *Arabian J. Chem.*, 10 (2017) 3229–3238.
- [12] P. Sivakumar, S. Deepalakshmi, A. Sircar, N. Yasvanthrajan, M.S. Shima, P. Sivakumar, Studies on three-phase three-dimensional hybrid electrochemical reactor for treating textile effluent, *Desal. Wat. Treat.*, 116 (2018) 242–250.
- [13] H.N. Bhatti, A. Jabeen, M. Iqbal, S. Noreen, Z. Naseem, Adsorptive behavior of rice bran-based composites for malachite green dye: isotherm, kinetic and thermodynamic studies, *J. Mol. Liq.*, 237 (2017) 322–333.
- [14] R.H. Hesas, A. Arami-Niya, W.M.A.W. Daud, J.N. Sahu, Preparation and characterization of activated carbon from apple waste by microwave-assisted phosphoric acid activation: application in methylene blue adsorption, *BioResources*, 8 (2013) 2950–2966.
- [15] D. Suteu, T. Malutan, D. Bilba, Agricultural waste corn cob as a sorbent for removing reactive dye orange 16: equilibrium and kinetic study, *Cellul. Chem. Technol.*, 45 (2011) 413–420.
- [16] S. De-Gisi, G. Lofrano, M. Grassi, M. Notarnicola, Characteristics and adsorption capacities of low-cost sorbents for wastewater treatment: a review, *Sustainable Mater. Technol.*, 9 (2016) 10–40.
- [17] S.C. Santos, A.F. Oliveira, R.A. Boaventura, Bentonitic clay as adsorbent for the decolourisation of dye house effluents, *J. Cleaner Prod.*, 126 (2016) 667–676.
- [18] D.B. Jirekar, A.A. Pathan, M. Farooqui, Adsorption studies of methylene blue dye from aqueous solution onto *Phaseolus aureus* biomaterials, *Orient. J. Chem.*, 30 (2014) 1263–1269.
- [19] S. Noreen, H.N. Bhatti, M. Zuber, M. Zahid, M. Asgher, Removal of actacid orange-RL dye using biocomposites: modeling studies, *Pol. J. Environ. Stud.*, 26 (2017) 2125–2134.
- [20] N. Praveena, P. Saravanan, S.D. Kumar, N.N. Gandhi, S. Renganathan, Biosorption of reactive red 198 from an aqueous solution using *Acalypha indica*, *Asia-Pac. J. Chem. Eng.*, 7 (2011) 761–768.
- [21] M. Bilal, H.M. Iqbal, H. Hu, W. Wang, X. Zhang, Enhanced bio-catalytic performance and dye degradation potential of chitosan-encapsulated horseradish peroxidase in a packed bed reactor system, *Sci. Total Environ.*, 575 (2017) 1352–1360.
- [22] K.I. Andersson, M. Eriksson, M. Norgren, Lignin removal by adsorption to fly ash in waste water generated by mechanical pulping, *Ind. Eng. Chem. Res.*, 51 (2012) 3444–3451.
- [23] E. Rashedi, H. Nezamabadi-Pour, S. Saryazdi, GSA: a gravitational search algorithm, *Inf. Sci.*, 179 (2009) 2232–2248.
- [24] H.P. Boehm, Chemical identification of surface groups, *Adv. Catal.*, 16 (1966) 179–274.
- [25] G. Sposito, On points of zero charge, *Environ. Sci. Technol.*, 32 (1998) 2815–2819.
- [26] H. Bessaha, M. Bouraada, L.C. de Ménorval, Removal of an acid dye from water using calcined and uncalcined ZnAl-r anionic clay, *Water Environ. Res.*, 89 (2017) 783–790.
- [27] R. Wang, Y. Chu, M. Chen, Adsorption kinetics of ¹³⁷Cs⁺/⁹⁰Sr²⁺ on Ca-Bentonite, *Water Environ. Res.*, 89 (2017) 791–797.
- [28] S. Mandal, M.K. Sahu, R.K. Patel, Adsorption studies of arsenic (III) removal from water by zirconium polyacrylamide hybrid material (ZrPACM-43), *Water Resour. Ind.*, 4 (2013) 51–67.
- [29] I.I. Salame, T.J. Bandosz, Surface chemistry of activated carbons: combining the results of temperature-programmed desorption, Boehm, and potentiometric titrations, *J. Colloid Interface Sci.*, 240 (2001) 252–258.
- [30] D. Pathania, S. Sharma, P. Singh, Removal of methylene blue by adsorption onto activated carbon developed from *Ficus carica* bast, *Arabian J. Chem.*, 10 (2017) 1445–1451.
- [31] M. Moyo, L. Chikazaza, B.C. Nyamunda, B.U. Guyo, Adsorption batch studies on the removal of Pb (II) using maize tassel based activated carbon, *J. Chem.*, 2013 (2013) 1–8.
- [32] W. Peng, H. Li, Y. Liu, S. Song, A review on heavy metal ions adsorption from water by graphene oxide and its composites, *J. Mol. Liq.*, 230 (2017) 496–504.
- [33] J.S. Piccin, C.S. Gomes, L.A. Feris, M. Gutierrez, Kinetics and isotherms of leather dye adsorption by tannery solid waste, *Chem. Eng. J.*, 183 (2012) 30–38.
- [34] F.C. Wu, R.L. Tseng, R.S. Juang, Characteristics of Elovich equation used for the analysis of adsorption kinetics in dye-chitosan systems, *Chem. Eng. J.*, 150 (2009) 366–373.
- [35] G. Nazari, H. Abolghasemi, M. Esmaili, E.S. Pouya, Aqueous phase adsorption of cephalixin by walnut shell-based activated carbon: a fixed-bed column study, *Appl. Surf. Sci.*, 375 (2016) 144–153.
- [36] H. Beheshti, M. Irani, L. Hosseini, A. Rahimi, M. Aliabadi, Removal of Cr (VI) from aqueous solutions using chitosan/MWCNT/Fe₃O₄ composite nanofibers -batch and column studies, *Chem. Eng. J.*, 284 (2016) 557–564.